HHS Public Access

Author manuscript

ACS Nano. Author manuscript; available in PMC 2019 April 18.

Published in final edited form as:

ACS Nano. 2018 December 26; 12(12): 12193–12200. doi:10.1021/acsnano.8b05892.

Pretargeting and Bioorthogonal Click Chemistry-Mediated Endogenous Stem Cell Homing for Heart Repair

Zhenhua Li[#†,‡], **Deliang Shen**[#§], **Shiqi Hu**[#†,‡], **Teng Su**[†,‡], **Ke Huang**[†,‡], **Feiran Liu**[†,‡], **Lei Hou**[*,‖,⊥], and **Ke Cheng**[*,†,‡]

[†]Department of Molecular Biomedical Sciences and Comparative Medicine Institute, North Carolina State University, Raleigh, North Carolina 27607, United States

[‡]Joint Department of Biomedical Engineering, University of North Carolina at Chapel Hill, Chapel Hill, North Carolina 27599, and North Carolina State University, Raleigh, North Carolina 27695, United States

[§]Department of Cardiology, The First Affiliated Hospital of Zhengzhou University, Zhengzhou, Henan 450052, China

[‖]Department of Cardiology, Tongren Hospital, Shanghai Jiaotong University School of Medicine, Shanghai 200336, China

[⊥]Department of Cardiology, Shanghai Institute of Cardiovascular Diseases, Zhongshan Hospital, Fudan University, Shanghai 200433, China

[#] These authors contributed equally to this work.

Abstract

Stem cell therapy is one of the promising strategies for the treatment of ischemic heart disease. However, the clinical application of stem cells transplantation is limited by low cell engraftment in the infarcted myocardium. Taking advantage of pretargeting and bioorthogonal chemistry, we engineered a pretargeting and bioorthogonal chemistry (PTBC) system to capture endogenous circulating stem cells and target them to the injured heart for effective repair. Two bioorthogonal antibodies were i.v. administrated with a pretargeting interval (48 h). Through bioorthogonal click reaction, the two antibodies are linked *in vivo*, engaging endogenous stem cells with circulating platelets. As a result, the platelets redirect the stem cells to the injured heart. *In vitro* and *in vivo* studies demonstrated that bioorthogonal click reaction was able to induce the conjugation of platelets and endothelial progenitor cells (EPCs) and enhance the binding of EPCs to collagen and

[*]**Corresponding Authors:** houlei@fudan.edu.cn., ke_cheng@ncsu.edu.

Author Contributions

Z.L. and K.C. conceived the study; Z.L., D.S., S.H., T.S., K.H., and F.L. performed the experiments and collected data; Z.L., L.H., and K.C. wrote the paper; L.H. and K.C. provided financial support.

ASSOCIATED CONTENT

Supporting Information

The Supporting Information is available free of charge on the ACS Publications website at DOI: 10.1021/acsnano.8b05892.

Description of animal models, SDS-PAGE experiments, immunofluorescence imaging, TEM and SEM imaging, aggregometry assay, histological analysis, and histochemistry (PDF)

Notes

The authors declare no competing financial interest.

injured blood vessels. More importantly, in a mouse model of acute myocardial infarction, the *in vivo* results of cardiac function, heart morphometry, and immunohistochemistry assessment all con*fi*rmed e*ff*ective heart repair by the PTBC system.

Graphical Abstract

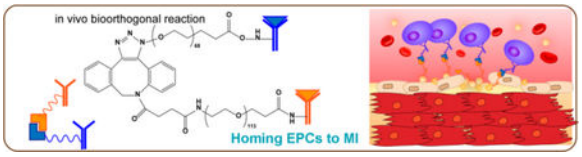

Keywords

pretargeting; bioorthogonal click chemistry; heart repair; endogenous stem cells; engineered antibodies

Acute myocardial infarction (AMI) remains a leading cause of mortality and morbidity around the world.[1] During an AMI, blood flow to the heart muscle is abruptly cut off, causing death of cardiomyocytes. A major MI can subsequently lead to heart failure. Once failure occurs, the only option left is heart transplantation.[2] Cardiac cell therapy is a promising option, yet its clinical efficacy has been marginal due at least in part to low cell engraftment and entrapment in the lung after intravenous delivery.[3–6] In the meanwhile, endogenous stem cells are released from the bone marrow as a natural response to the MI injury.[7] However, this natural repair process is insufficient because of inadequate homing of the stem cells to the injured heart, even in the presence of bone-marrow-stimulating agents such as granulocyte colony-stimulating factor (G-CSF).[8,9]

We designed a pretargeting/bioorthogonal conjugation (PTBC) system to achieve endogenous cell-mediated heart repair without cellular transplantation (Scheme 1). Bioorthogonal click reaction is extremely selective, versatile, and biocompatible and has been indicated as an efficient chemical reaction for numerous biological applications.[10–12] CD34 antibodies (binding to endogenous stem cells) and CD41 antibodies (binding to platelets, which target the MI area) were first modified using bioorthogonal azide and dibenzocyclooctyne (DBCO) attached poly(ethylene glycol) (PEG) derivative, respectively. Next, to address the limitations of bispecific antibodies (BsAb), we introduce the concept of pretargeting, in which these two bioorthogonal antibodies were i.v. administrated with a pretargeting interval (48 h): CD41 attached DBCO polymer (DBCO-PEG-CD41) will pretarget platelets and inherently accumulate on the MI area owing to the homing ability of platelets.[13,14] After the pretargeting interval, azide-modified CD34 (Az-PEG-CD34) is given and will recognize and bind to endogenous stem cells. Then azide groups on the stem cells will recognize and react with DBCO groups on platelets. Thus, *via* bioorthogonal click reaction, endogenous stem cells are engaged with platelets. The attached platelets will “piggyback” the stem cells and accumulate them in the infarcted area for cardiac repair. Our PTBC system will provide a theoretical and experimental foundation in the field of heart disease therapy.

RESULTS AND DISCUSSION

Fabrication of Bioorthogonal Antibodies.

Pretargeting and bioorthogonal capturing antibodies were produced by covalent conjugation of antibodies to two bioorthogonal hetero PEG derivatives (DBCO-PEG-NHS and Azide-PEG-NHS). DBCO and azide groups were chosen because they are extremely selective. Since CD41 antibodies could bind to platelets, we first conjugated CD41 antibodies with DBCO-PEG-NHS and obtained a pretargeting group (DBCO-PEG-CD41). CD34 antibodies, recognizing circulating CD34-positive stem cells, were reacted with Az-PEG-NHS to give bioorthogonal capturing antibodies (Az-PEG-CD34). SDS-PAGE was performed to confirm the successful conjugations (Figure 1A). Polymer-modified antibodies ran slowly, and both the DBCO-PEG-CD41 and Az-PEG-CD34 antibody−polymer conjugations were determined by the absence of discrete free protein bands in the SDS-PAGE gels in contrast to native antibodies. In addition, to prove the targeting capability of CD34 and CD41, we also generated two bioorthogonal IgG−polymer building blocks as negative controls (Figures S1 and S2). Moreover, we directly conjugated DBCO-PEG-CD41 with Az-PEG-CD34 to generate BsAb, as another control agent. SDS-PAGE results showed a low mobility, confirming the presence of BsAb. Furthermore, CD34 and CD41 antibodies with different sources were bioorthogonally conjugated, and we could use gold nanoparticle-labeled secondary antibody to detect BsAb. As shown in Figure S3, the presence of 10 nm gold nanoparticles around the surface of 40 nm gold nanoparticles suggested successful click reaction.

Characterization of Bioorthogonal Conjugation *in Vitro*.

We then confirmed that polymer-modified antibodies showed excellent immunoreactivity and could mediate bioorthogonal conjugation by click reaction. We first tested if the Az-PEG-CD34 could bind to CD34-positive cells and generate Az groups on the surface of stem cells. Endothelial progenitor cells (EPCs) were incubated with Az-PEG-CD34. And then Alexa Fluor 647 DIBO alkyne and DBCO-attached gold nanoparticles (40 nm) were used to detect Az groups. Alexa Fluor 647 fluorescence could be detected on the membrane of EPCs (Figure 1B). In contrast, Alexa Fluor 647 DIBO alkyne alone could not stain the EPCs. In addition, DBCO-labeled gold nanoparticles (40 nm) were also synthesized to detect the Az groups on EPCs using scanning electron microscopy (SEM) (Figure 1C). Fluorescein (FAM) azide was then introduced to test the DBCO groups on the cell surface. As expected, DBCO-PEG-CD41-treated platelets displayed DBCO groups on the surface (Figure S4). Finally, the direct conjugation of platelets and EPCs mediated by bioorthogonal Az-PEG-CD34 and DBCO-PEG-CD41 was confirmed using cryo-SEM and SEM. As shown in Figures 1D and S5, SEM images revealed that Az-PEG-CD34-pretreated EPCs were indeed covered with DBCO-PEG-CD41-treated platelets. Microscopy images were consistent with the SEM results, as there was an overlay between DiI (1,1’-dioctadecyl-3,3,3’,3’-tetramethylindocarbocyanine per-chlorate) (red, EPCs) and DiO (3,3′-dioctadecyloxacarbocyanine perchlorate) (green, platelets), suggesting that platelets were attached to EPCs (Figure S6). As a control, platelets without pretreatment showed minimal binding to EPCs. These compound data sets confirmed that the pretargeting DBCO groups

on platelets could be efficiently captured by Az-PEG-CD34-treated EPCs through bioorthogonal click reaction.

Assessment of Binding Ability.

To test the potency of the PTBC system *in vitro*, we evaluated EPC attachment on human umbilical vein endothelial cells (HUVECs) and collagen-coated surfaces (Figure S7A and B). We found that the phosphate-buffered saline (PBS), DBCO-PEG-CD41&Az-PEG-IgG (only pretargeting, PT), and DBCO-PEG-IgG&Az-PEG-CD34 (no pretargeting but only bioorthogonal conjugation, BC) groups exhibited only negligible levels of binding to collagen-coated surfaces. In contrast, PTBC produced a robust binding efficiency to collagen-coated surfaces. We also tested PTBC using *ex vivo* injured blood vessels. Mice aorta was isolated and surgically scraped to expose the subendothelial matrix. Figure S7C shows negligible DiI-labeled EPCs were bound to control (nondenuded) aortas. As expected, the PTBC system induced an efficient binding to denuded aorta in contrast to other control groups (Figure S7D). Similar results were confirmed in the presence of whole blood (Figure S7E).

Homing of Endogenous Stem Cells to the Infarct by PTBC.

Before animal studies, we further tested whether our PTBC system is pro-thrombotic. From the aggregometry results, we found the presence of PTBC did not cause thrombosis (Figure S8). We then went ahead to test the safety and efficacy of PTBC in a rodent model of AMI. It is well established that cytokines/growth factors such as G-CSF or VEGF can stimulate the release of CD34-positive stem cells from the bone marrow into the circulation.[15,16] To maximize the numbers of EPCs for targeting, G-CSF was preadministrated before PTBC treatment (Figure 2A). Increases in CD34-positive cells in the blood were confirmed (Figure 2B). We then evaluated the targeted binding ability of DBCO-PEG-CD41 to platelets *in vivo*. The enhanced accumulation in the MI area owing to the injury-homing ability of platelets was demonstrated. Cy5-Az was used as a detection probe, and Figure 2C and D show most of the DBCO groups were found to accumulate on the heart tissue, indicating that platelets transported the attached DBCO-PEG-CD41 to MI and reacted with Cy5-Az. As a control, administrating Cy5-Az alone resulted in the accumulation of dyes on the kidney, which was mainly attributed to the renal clearance of small molecules. These results indicated that DBCO-PEG-CD41 had the ability to bind to platelets *in vivo* and accumulated on the MI area. Furthermore, to confirm the PTBC system was superior to the traditional stem-cell-based therapeutic method, we also performed i.v. injection of DiR-labeled and Az group anchored EPCs. As shown in Figure 2E and F, the EPCs mainly remained in the lung, which was consistent with previous work in which stem cells were easily trapped in the lungs after i.v. injection. In addition, we also found large assemblies were formed owing to the surplus of DBCO groups on platelets and Az groups on EPCs. Platelets and stem cells may conjugate together and clog the blood vessels (Figure S9).

Therapeutic Effects of PTBC in a Mouse Model of MI.

To test the therapeutic potential of our PTBC system *in vivo*, MI mice were randomized into four groups with various treatments (Figure 3A). Previous work indicated that adult cardiomyocytes had extremely limited capacity to proliferate *in vivo*.[17] Ki67 was expressed

in cycling cells in G1, S, G2, and early mitosis.[18] A large number of cardiomyocytes (CM) underwent proliferation and cell cycle re-entry within the infarct region after PTBC treatment (Figure 3B and C). Interestingly, PTBC treatment showed a higher ability to promote CM proliferation (about 2.5-fold) than that of the BsAb group. Furthermore, von Willebrand Factor (vWF) were also stained to analyze microvascular angiogenesis. As could be seen in Figure 3D and E, we found the number of blood vessels increased in the scar area of the heart, indicating that infusion of PTBC promoted angiogenesis in the post-MI heart. In addition, cardiac morphology, fibrosis, and pump function were also evaluated. Left ventricular ejection fractions (LVEFs) and farctional shortening (FS) were measured at baseline (4 h postinfarct) and 4 weeks afterward (Figure 3F and G). In addition, echocardiography measurement analysis was performed, and the results showed significantly improved LVEF and FS values in the PTBC-treated mice compared to control groups at 4 weeks post-MI. Masson's trichrome-staining revealed significantly attenuated interstitial and perivascular fibrosis compared with control-injected hearts (Figure 4A and B). Moreover, susceptible organs including liver, spleen, lung, and kidney were unaffected after treatment with PTBC, indicating good biocompatibility of the system (Figure S10). Taken together, these data suggested the regenerative/reparative potential of the PTBC system for treating ischemic heart diseases.

Mechanisms Underlying the Therapeutic Benefits of PTBC.

Finally, to study the possible mechanisms underlying the therapeutic benefits of PTBC, DBCO-PEG-CD41-pretargeted hearts were harvested after 48 h, and their distribution in the injured hearts was studied using FAM-Az. Figure 4C and D show a large amount of green fluorescence from conjugated FAM was detected in the infarct region, which indicated the DBCO-PEG-CD41 might be transported by the MI-homing platelets. To further confirm our hypothesis that more endogenous stem cells were accumulated on the MI area treated by our PTBC system, the number of CD34-positive cells was analyzed (Figure 4E and F). Immunofluorescence staining indicated that endogenous CD34 cells were recruited to the infarcted heart. Pretargeting antibodies were first bound to platelets and transported to MI, and then capturing antibodies bound to endogenous CD34 cells helped engage the CD34 cells with platelets in the infarcted heart. Moreover, PTBC administration did not exacerbate the infiltration of CD8-positive T cells and CD68-positive macrophages in the post-MI heart (Figure S11 and Figure S12).

CONCLUSIONS

Targeting therapeutic cells to the infarcted heart has been a challenging practice.[19–21] Previously, our group has employed multiple modalities to tackle this problem, from magnetic targeting strategies[22,8] to peptide targeting,[23] and more recently to the uses of biomimetic approaches utilizing the binding motif on platelets.[14,24] Taking advantage of pretargeting and bioorthogonal chemistry, here we designed a two-step capturing strategy to recruit endogenous stem cells to the injured heart. Several aspects of our study are innovative. First, pretargeting, which was originally developed for tumor immunoscintigraphy to improve tumor-to-normal tissue contrast ratios, was introduced into the practice of regenerative medicine and endogenous cell therapy; second, bioorthogonal

chemistry with highly selective, versatile, and biocompatible properties would ensure the second capturing antibodies efficiently reacted with DBCO groups in the infarct heart; third, invasive intramyocardial injections were avoided by relying on the homing of endogenous cells; last but not the least, PTBC was a cell-free capturing and homing system, and lung entrapment seen in conventional intravenous cell therapy could be avoided. Our study provided a promising cell-free approach to promote myocardial repair after acute MI. However, our study had several limitations. The use of whole antibody may provoke an immune reaction of the body owing to the presence of Fc fragments. Future studies should focus on more biocompatible agents such as Fab and ScFv to construct the PTBC system. For clinic applications, most of the acute MI patients would receive percutaneous coronary intervention (PCI) to dredge the occluded coronary artery. Combining the traditional PCI with our PTBC system may induce a higher therapeutic efficiency, as PCI reanalyzed the culprit vessel while the PTBC system recruited stem cells to the infarct for effective post-MI repair.

EXPERIMENTAL SECTION

Fabrication of CD34 and CD41 Bioorthogonal Antibodies.

CD34 and CD41 antibodies were first reacted with Az-PEG-NHS and DBCO-PEG-NHS by $-NH_2$ and NHS acylation reaction. Equimolar CD34 and Az-PEG-NHS or CD41 and DBCO-PEG-NHS were mixed together and reacted at 4 °C for 24 h. Then the unreacted Az-PEG-NHS and DBCO-PEG-NHS were removed by centrifugation using an Amicon Ultra-0.5 filter (100 kDa) to give the bioorthogonal Az-PEG-CD34 and DBCO-PEG-CD41. The bispecific antibodies were also synthesized as a control. The successful conjugation was proved using SDS-PAGE and transmission electron microscopy (TEM).

Confirmation of Binding Ability to EPCs.

A total of 1×10^4 CD34-positive EPCs (Cell Biologics, Chicago, IL, USA) were seeded on four-well culture chamber slides and stained using DiO. Then 2 μg of Az-PEG-CD34 was mixed with EPCs for 4 h. The group without Az-PEG-CD34 was also carried out as a control. After incubation, the cells were then washed three times with PBS, Alexa Fluor 647 DIBO alkyne (2 μg) was added, and the mixture was incubated for another 1 h. After incubation, the cells were then washed with PBS three times, 500 μL of fixing solution was added to each well for 30 min, and finally the images were captured using a Nikon confocal fluorescent microscope. To further confirm the presence of azide groups on the surface of EPCs after Az-PEG-CD34 binding, DBCO-labeled gold nanoparticles (40 nm) were added to recognize and react with azide groups on EPCs. After 1 h of incubation, the unreacted DBCO-labeled gold nanoparticles were removed, the EPCs were dehydrated gradually, and cells were imaged by SEM. The DBCO-labeled gold nanoparticles were obtained from the reaction of amino-modified gold nanoparticles with DBCO-PEG-NHS.

Confirmation of Binding Ability to Platelets.

Murine platelets were isolated as we have described previously. A total of 10^6 platelets were incubated with 2 μg of DBCO-PEG-CD41 at 37 °C for 2 h. The unbound DBCO-PEG-CD41 was removed by centrifugation at 600*g* for 8 min. The presence of DBCO groups was

reacted with an azide-modified fluorescent dye, FAM-Az, and detected using a Nikon fluorescent microscope.

Conjugation of P-DBCO to EPC-Az.

The biorthogonal conjugation of platelets to EPCs was then conducted. P-DBCO and EPC-Az were mixed together and incubated at 37 °C for 2 h. The unbound P-DBCO was removed by centrifugation at 400*g* for 3 min. The P-EPC was imaged by both SEM and cryo-SEM. In addition, we also confirmed the bioorthogonal conjugation of platelets to EPCs using fluorescent microscopy. P-DBCO was labeled with DiO, and the EPC-Az was seeded on four-well slides, stained with DiI, and then mixed together. After 2 h, the unreacted P-DBCO underwent centrifugation at 600*g* for 8 min and removed by centrifugation at 400*g* for 3 min. The platelet-attached EPCs were detected using a Nikon fluorescent microscope.

Collagen Surface Binding Assay.

GFP-tagged HUVECs (Angio-Proteomie, Boston, MA, USA) were cultured on collagen-coated slides according to our previous work.[14] Platelets (10^6) were first added to all chambers. We designed four groups to show the enhanced binding efficiency using PTBC systems. (1) DBCO-PEG-CD41 was added and incubated for 30 min. After removing the unattached DBCO-PEG-CD41, Az-PEG-CD34 was mixed for another 30 min. Finally, DiI-labeled EPCs were added. (2) DBCO-PEG-CD41 was added and incubated for 30 min. After washing with PBS, Az-PEG-IgG was added and incubated for another 30 min. Finally, DiI-labeled EPCs were added. (3) DBCO-PEG-IgG was added and incubated for 30 min. After removing the unattached DBCO-PEG-IgG, Az-PEG-IgG were mixed for another 30 min. Finally, DiI-labeled EPCs were added. (4) EPCs were added alone. Next, the cells were imaged using fluorescence microscopy. Attached EPCs were quantified.

Denuded Aorta Binding Assay.

To test enhanced binding of EPCs on denuded vascular by PTBC systems, C57BL/6 mice aortas were dissected and surgically scraped on their luminal side with forceps to remove the endothelial layer. Platelets (106) were first added to control or denuded aortas. We designed four groups to show the enhanced binding efficiency using PTBC systems. (1) DBCO-PEG-CD41 was mixed for 30 min. After removing the unattached DBCO-PEG-CD41, Az-PEG-CD34 was added for another 30 min. Finally, DiI-labeled EPCs were added. (2) DBCO-PEG-CD41 was incubated for 30 min followed by washing with PBS. Az-PEG-IgG were then incubated for another 30 min. Finally, DiI-labeled EPCs were added. (3) DBCO-PEG-IgG were mixed for 30 min. After washing with PBS, Az-PEG-IgG were mixed for another 30 min. Finally, DiI-labeled EPCs were added. (4) EPCs were added alone. Both injured and normal aortas were mixed with DiI-labeled P-EPC or EPCs for 5 min. After PBS washing, samples were taken using fluorescence microscopy for the examination of cell binding.

G-CSF Treatment for CD34 Cell Release.

C57 mice were i.v. given G-CSF (50 μg/day, $n = 4$ animals per group). After 1 and 2 d intervals, the blood was drawn and the red blood cells were lysed. FITC-tagged anti-mouse

CD34 antibodies (eBioscience) were then used to stain CD34-positive stem cells analyzed using FACS.

Evaluation of PTBC's Capturing Ability in Whole Blood.

In brief, whole blood was collected from the C57BL/6 mice. The Az-PEG-CD34 attached EPCs (10^5) were then stained using DiD and mixed with 1 mL of whole blood. Then PBS, DiO-labeled platelets, and DBCO-PEG-CD41-pretreated DiO-labeled platelets were mixed for 30 min. Then RBCs were lysed, and the samples were analyzed using flow cytometry.

Supplementary Material

Refer to Web version on PubMed Central for supplementary material.

ACKNOWLEDGMENTS

This work was supported by grants from the National Institutes of Health (HL123920 and HL137093 to K.C.), American Heart Association (18TPA34230092 to K.C.), and the National Natural Science Foundation of China (81770254 to L.H. and 81873493 to D.S.). This work was performed in part at the Analytical Instrumentation Facility (AIF) at North Carolina State University, which is supported by the State of North Carolina and the National Science Foundation (award number ECCS-1542015). The AIF is a member of the North Carolina Research Triangle Nanotechnology Network (RTNN), a site in the National Nanotechnology Coordinated Infrastructure (NNCI).

REFERENCES

(1). Wang M; Vaez M; Dorner TE; Tiihonen J; Voss M; Ivert T; Mittendorfer-Rutz E Trajectories and Characteristics of Work Disability Before and After Acute Myocardial Infarction. Heart 2018, 104, 340–348. [PubMed: 28864716]

(2). Hashimoto H; Olson EN; Bassel-Duby R Therapeutic Approaches for Cardiac Regeneration and Repair. Nat. Rev. Cardiol 2018, 15, 585–600. [PubMed: 29872165]

(3). Tongers J; Losordo DW; Landmesser U Stem and Progenitor Cell-based Therapy in Ischaemic Heart Disease: Promise, Uncertainties, and Challenges. Eur. Heart J 2011, 32, 1197–1206. [PubMed: 21362705]

(4). Menasché P Cell Therapy Trials for Heart Regeneration — Lessons Learned and Future Directions. Nat. Rev. Cardiol 2018, 15, 659–671. [PubMed: 29743563]

(5). Lin Z; Pu WT Strategies for Cardiac Regeneration and Repair. Sci. Transl. Med 2014, 6, 239rv1–239rv1.

(6). Tang J; Cui X; Caranasos TG; Hensley MT; Vandergriff AC; Hartanto Y; Shen D; Zhang H; Zhang J; Cheng K Heart Repair Using Nanogel-Encapsulated Human Cardiac Stem Cells in Mice and Pigs with Myocardial Infarction. ACS Nano 2017, 11, 9738–9749. [PubMed: 28929735]

(7). Pacelli S; Basu S; Whitlow J; Chakravarti A; Acosta F; Varshney A; Modaresi S; Berkland C; Paul A Strategies to Develop Endogenous Stem Cell-recruiting Bioactive Materials for Tissue Repair and Regeneration. Adv. Drug Delivery Rev 2017, 120, 50–70.

(8). Cheng K; Shen D; Hensley MT; Middleton R; Sun B; Liu W; De Couto G; Marbań E Magnetic Antibody-linked Nano-matchmakers for Therapeutic Cell Targeting. Nat. Commun 2014, 5, 4880–4888. [PubMed: 25205020]

(9). Bianconi V; Sahebkar A; Kovanen P; Bagaglia F; Ricciuti B; Calabrò P; Patti G; Pirro M Endothelial and Cardiac Progenitor Cells for Cardiovascular Repair: A Controversial Paradigm in Cell Therapy. Pharmacol. Ther 2018, 181, 156–168. [PubMed: 28827151]

(10). Li Z; Liu Z; Chen Z; Ju E; Li W; Ren J; Qu X Bioorthogonal Chemistry for Selective Recognition, Separation and Killing Bacteria Over Mammalian Cells. Chem. Commun 2016, 52, 3482–3485.

(11). Pan H; Zhang P; Gao D; Zhang Y; Li P; Liu L; Wang C; Wang H; Ma Y; Cai L Noninvasive Visualization of Respiratory Viral Infection Using Bioorthogonal Conjugated Near-Infrared-Emitting Quantum Dots. ACS Nano 2014, 8, 5468–5477. [PubMed: 24797178]

(12). Du L; Qin H; Ma T; Zhang T; Xing D In Vivo Imaging-Guided Photothermal/Photoacoustic Synergistic Therapy with Bioorthogonal Metabolic Glycoengineering-Activated Tumor Targeting Nanoparticles. ACS Nano 2017, 11, 8930–8943. [PubMed: 28892360]

(13). Ziegler M; Wang X; Lim B; Leitner E; Klingberg F; Ching V; Yao Y; Huang D; Gao X-M; Kiriazis H; Du X-J; Haigh JJ; Bobik A; Hagemeyer CE; Ahrens I; Peter K Platelet-Targeted Delivery of Peripheral Blood Mononuclear Cells to the Ischemic Heart Restores Cardiac Function after Ischemia-Reperfusion Injury. Theranostics 2017, 7, 3192–3206. [PubMed: 28900504]

(14). Tang J; Su T; Huang K; Dinh P-U; Wang Z; Vandergriff A; Hensley MT; Cores J; Allen T; Li T; Sproul E; Mihalko E; Lobo LJ; Ruterbories L; Lynch A; Brown A; Caranasos TG; Shen D; Stouffer GA; Gu Z; Zhang J; Cheng K Targeted Repair of Heart Injury by Stem Cells Fused with Platelet Nanovesicles. Nat. Biomed. Eng 2018, 2, 17–26. [PubMed: 29862136]

(15). Goldstein L; Gallagher K; Bauer S; Bauer R; Vijay B; Zhao-Jun L; G, B. D.; R, T. S.; C, V. O. Endothelial Progenitor Cell Release into Circulation Is Triggered by Hyperoxia-Induced Increases in Bone Marrow Nitric Oxide. Stem Cells 2006, 24, 2309–2318. [PubMed: 16794267]

(16). Vasa M; Fichtlscherer S; Adler K; Aicher A; Martin H; Zeiher AM; Dimmeler S Increase in Circulating Endothelial Progenitor Cells by Statin Therapy in Patients With Stable Coronary Artery Disease. Circulation 2001, 103, 2885–2890. [PubMed: 11413075]

(17). Mohamed TMA; Ang Y-S; Radzinsky E; Zhou P; Huang Y; Elfenbein A; Foley A; Magnitsky S; Srivastava D Regulation of Cell Cycle to Stimulate Adult Cardiomyocyte Proliferation and Cardiac Regeneration. Cell 2018, 173, 104–116. [PubMed: 29502971]

(18). Al-Hazmi N; Turki A; Gareth W; Kai S; Raghad A-D DNA Replication Licensing Factor MCM2, Geminin, and Ki67 Define Proliferative State and Are Linked with Survival in Oral Squamous Cell Carcinoma. Eur. J. Oral Sci 2018, 126, 186–196. [PubMed: 29745471]

(19). Hu S; Ogle BM; Cheng K Body Builder: from Synthetic Cells to Engineered Tissues. Curr. Opin. Cell Biol 2018, 54, 37–42. [PubMed: 29704858]

(20). Li Z; Hu S; Cheng K Platelets and Their Biomimetics for Regenerative Medicine and Cancer Therapies. J. Mater. Chem. B 2018, 6, 7354–7365.

(21). Tang J-N; Cores J; Huang K; Cui X-L; Luo L; Zhang J-Y; Li T-S; Qian L; Cheng K Concise Review: Is Cardiac Cell Therapy Dead? Embarrassing Trial Outcomes and New Directions for the Future. Stem Cells Transl. Med 2018, 7, 354–359. [PubMed: 29468830]

(22). Vandergriff AC; Hensley TM; Henry ET; Shen D; Anthony S; Zhang J; Cheng K Magnetic Targeting of Cardio-sphere-derived Stem Cells with Ferumoxytol Nanoparticles for Treating Rats with Myocardial Infarction. Biomaterials 2014, 35, 8528–8539. [PubMed: 25043570]

(23). Vandergriff A; Huang K; Shen D; Hu S; Hensley MT; Caranasos TG; Qian L; Cheng K Targeting Regenerative Exosomes to Myocardial Infarction Using Cardiac Homing Peptide. Theranostics 2018, 8, 1869–1878. [PubMed: 29556361]

(24). Su T; Huang K; Ma H; Liang H; Dinh P-U; Chen J; Shen D; Allen TA; Qiao L; Li Z; Hu S; Cores J; Frame BN; Young AT; Yin Q; Liu J; Qian L; Caranasos TG; Brudno Y; Ligler FS; Cheng K Platelet-Inspired Nanocells for Targeted Heart Repair After Ischemia/Reperfusion Injury. Adv. Funct. Mater 2018, 1803567.

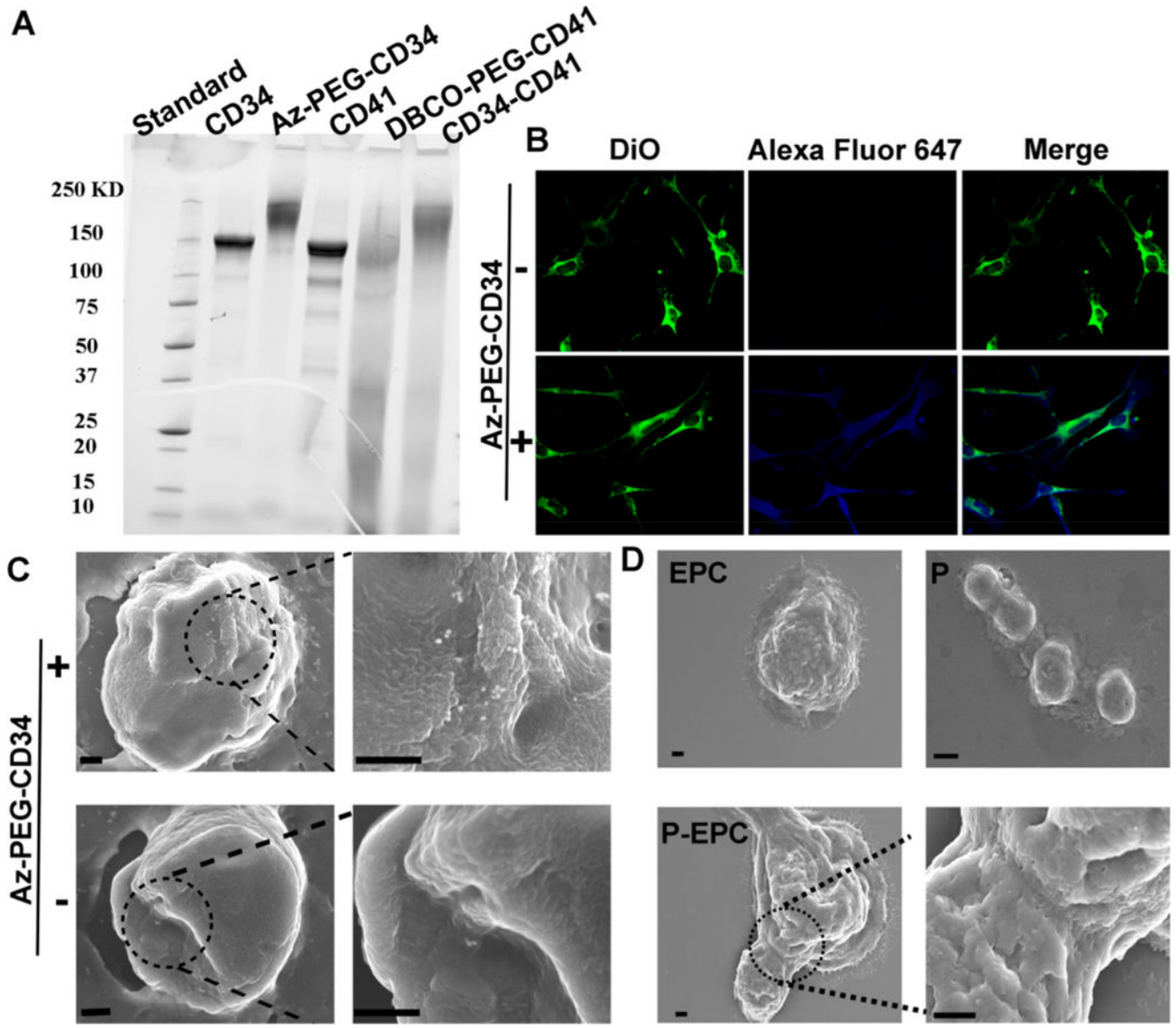

Figure 1.

Physiochemical and biological properties of bioorthogonal antibody-PEG derivatives. (A) SDS-PAGE. (B) Binding of Alexa Fluor 647 DIBO alkyne to the Az-PEG-CD34 attached EPCs. (C) SEM images of Az-PEG-CD34 attached EPCs and EPCs incubated with DBCO-PEG-modified gold nanoparticles. (D) SEM confirmed the conjugation of platelets to EPCs by click reaction. Scale bar, 20 μm for B, 0.5 μm for C, and 1 μm for D.

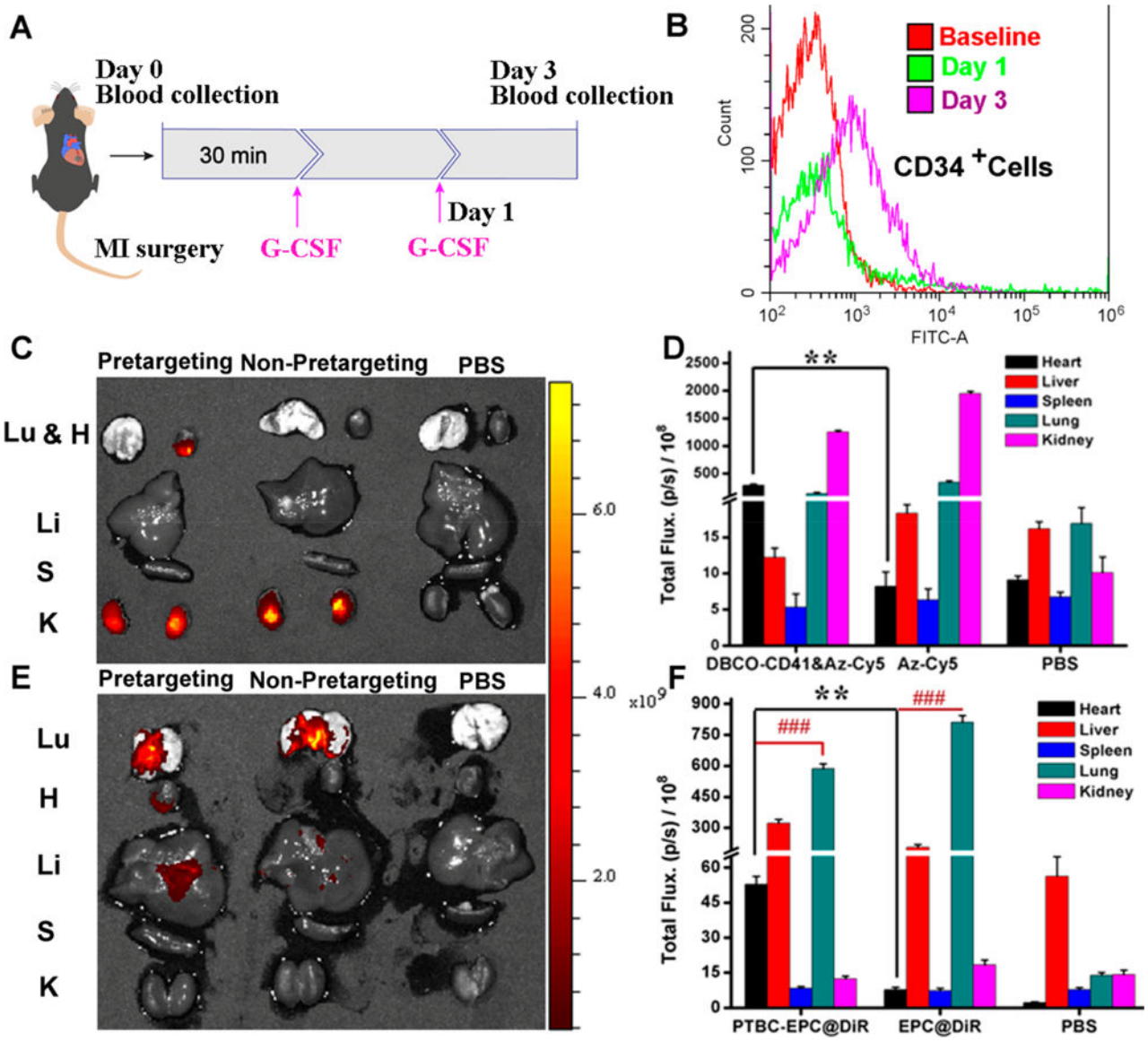

Figure 2.

Bioorthogonal reaction increases the homing of endogenous stem cells to the infarcted heart. (A) Schematic showing animal imaging study design. (B) Representative *flow* cytometry plot confirming the release of CD34-positive stem cells by G-CSF treatment. (C) *Ex vivo* fluorescent imaging of MI mice 48 h after i.v. injection of DBCO-PEG-CD41 followed with Cy5-Az (24 h interval), Cy5-Az alone, and PBS. (D) Quantitative anaysis. (E) *Ex vivo* fluorescent imaging of MI mice 48 h after i.v. injection of DBCO-PEG-CD41 followed with DiR-labeled EPCs (24 h interval), EPC-DiR alone, and PBS. (F) Quantitative analysis. Lu, H, Li, S, and K indicate the lung, heart, liver, spleen, and kidney, respectively, $n = 4$ animals per group, all data are mean ± SD. ** indicates $p < 0.01$; ### indicates $p < 0.005$.

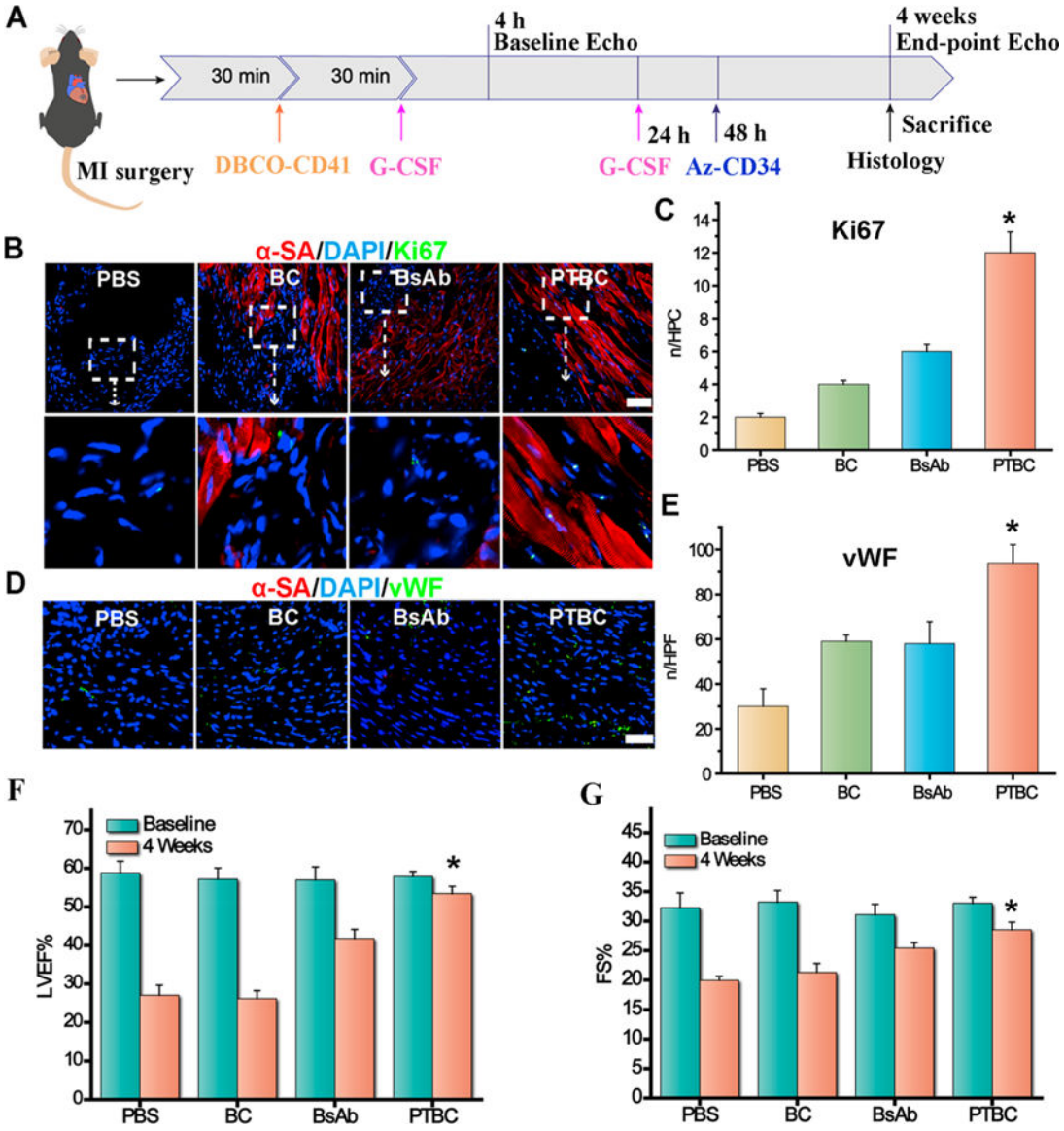

Figure 3.

PTBC treatment promotes angiomyogenesis and boosts cardiac function in mice with MI. (A) Schematic showing animal study design. (B) Images showing Ki67-positive cardiomyocyte nuclei in control PBS-, DBCO-PEG-IgG followed with Az-PEG-CD34 (BC), BsAb or DBCO-PEG-IgG followed with Az-PEG-CD34 (PTBC)-treated hearts. (C) Quantitative analysis of Ki67-positive nuclei. (D) Representative micrographs showing vWF-tagged vessels (green) treated by control PBS-, DBCO-PEG-IgG followed with Az-PEG-CD34 (BC), BsAb or DBCO-PEG-IgG followed with Az-PEG-CD34 (PTBC)-treated hearts at 4 weeks. (F, G) LVEFs and LVFSs measured by echo at baseline (4 h post-MI) and 4 weeks later ($n = 4$ animals per group). All data are mean ± SD. Scale bar, 40 μm. PTBC group *vs* the other three groups; * indicates $p < 0.05$.

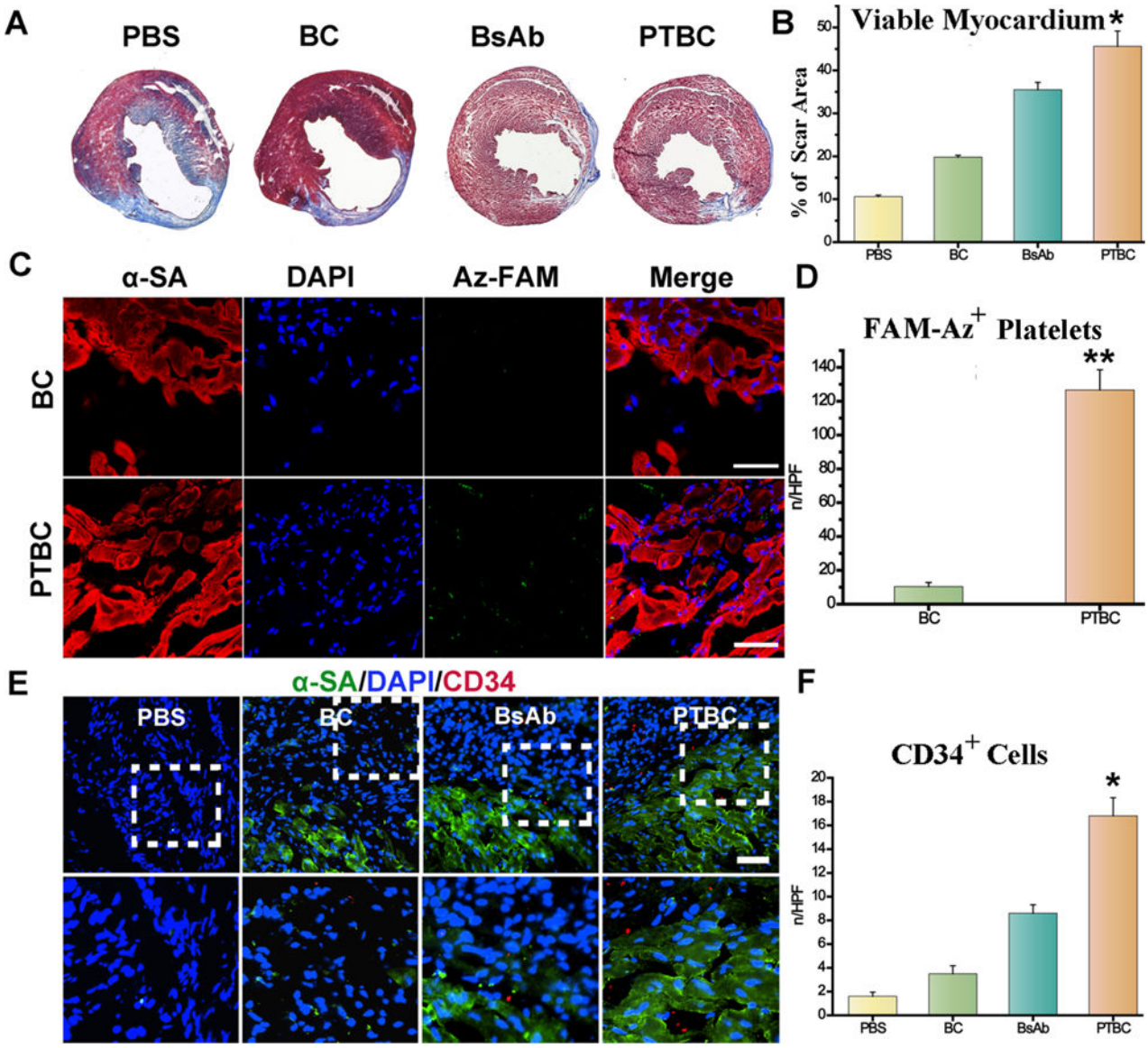

Figure 4.

PTBC enriches endogenous stem cells in the infarct and ameliorates ventricular remodeling. (A) Masson's Trichrome staining of heart sections 4 weeks after treatment. (B) Quantitative analysis of viable myocardium from the Masson's trichrome images. (C) Targeting ability of DBCO-PEG-IgG (BC) and DBCO-PEG-CD41 (PTBC) to MI. Scale bar, 50 μm. (D) Quantitative analysis of *fl*uorescent intensity from C. (E) Representative images showing CD34-positive cells in control PBS-, DBCO-PEG-IgG followed with Az-PEG-CD34 (BC), BsAb or DBCO-PEG-IgG followed with Az-PEG-CD34 (PTBC)-treated hearts at 4 weeks. (F) Quantitative analysis of the numbers of CD34-positive cells (n = 4 animals per group). All data are mean ± SD. Scale bar, 10 μm, PTBC group *vs* other groups, ** indicates $p <$ 0.01.

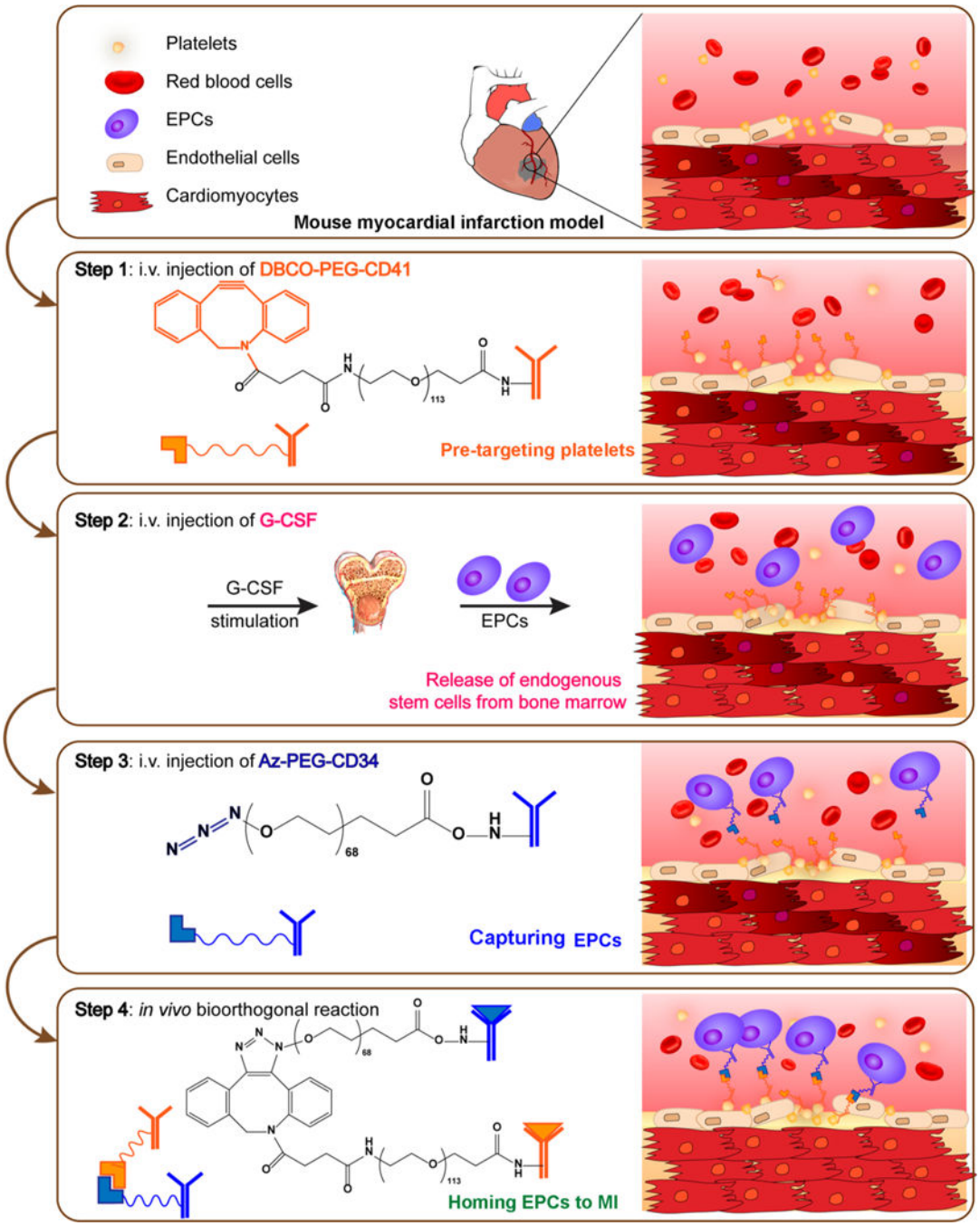

Scheme 1.
Schematic showing the synthesis of two bioorthogonal antibodies.